Journal of the European Ceramic Society **16** (1996) 515–519

0955-2219(95)00128-X
0955-2219/96/$15.00

Cavitation Induced by High-Temperature Plastic Deformation in Aluminium Nitride Ceramics

S. Choux,[a] I. Masson,[a,b] J. P. Feiereisen,[a] A. George[a] & J. P. Michel[a]

[a]Laboratoire Métallurgie Physique & Science des Matériaux (URA CNRS 155) and [b]Laboratoire Science et Génie des Matériaux Métalliques (URA CNRS 159), Ecole des Mines, Parc de Saurupt, 54042 Nancy Cedex, France

(Received 22 July 1994; revised version received 22 June 1995; accepted 14 July 1995)

Abstract

Intergranular cavitation has been investigated in samples deformed plastically up to a few per cent in four-point bending and uniaxial compression above 1500°C. Even for strains of 0·5%, cavities with a size of several tenths of a micrometre were observed, generally nucleated at small sintering additive particles. Cavities are preferentially formed in grain boundaries perpendicular to the stress axis in areas deformed in tension but are rather isotropically distributed in samples deformed in compression. The volume fraction of cavities was found to be near the total strain.

1 Introduction

Aluminium nitride is a stoichiometric compound of formula AlN. This ionocovalent material has an ionicity factor of 0·45 and a wurzite hexagonal crystalline structure (2 H with a = 0·311 nm and c = 0·498 nm). At room temperature AlN combines a high electrical resistivity (1×10^{13} Ω cm due to a band gap of 6·3 eV), an excellent thermal conductivity as high as 200 W m^{-1} K^{-1} and a low thermal expansion coefficient, ~2·7 $\times$ 10^{-6} K^{-1}, close to that of silicon. These properties and its non-toxicity make AlN a good candidate material for substrates of electronic devices. Also AlN exhibits a good thermal stability, does not react with molten metals and shows high mechanical strength up to 1500°C. It can therefore be used for some parts in a continuous casting process. This has prompted the present work on high-temperature plastic deformation of AlN ceramics. When undergoing creep at high-temperature, polycrystalline materials often fail as a result of the growth and coalescence of voids located at grain boundaries (GBs) to form cavities. We report here on cavitation in AlN.

2 Experimental Procedures

AlN powders are sintered with additives. The materials studied were provided by ESK (Germany) in two grades: conventionally sintered (hereafter called S-AlN) or hot-pressed (HP-AlN). In both cases, the additive was La_2O_3 (5 wt%). Equiaxial grains are observed with average sizes of 7 μm (S) and 4 μm (HP). The additive is found within the GBs and especially at triple grain junctions as particles of a few tenths of a micrometre. The as-received materials have no porosity.

Samples were deformed up to a few per cent plastic strain either by uniaxial compression, in creep under constant nominal stress of 150, 200 and 250 MPa or at a fixed strain rate, $\dot{\epsilon} \cong 5 \times 10^{-6}$ s^{-1}, or by four-point bending (FPB) under constant load. In the last case, the maximum stress on the outer fibres was equal to 58, 80 and 109 MPa.

Tests were performed under Ar + He atmosphere, at temperatures ranging from 1773 to 1923 K. Samples were cooled with the final stress applied in order to freeze-in microstructures and defects. Thin foils were then cut, thinned by ion-milling and observed in a Jeol 200 CX electron microscope operating at 200 kV. Further details can be found in Ref. 1.

3 Results

3.1 Influence of thermal treatment without applied stress

To separate the possible effects of heat treatment from those due to plastic deformation, observations were made on a sample heated for 5 h at the highest investigated temperature, 1923 K, without any applied stress. Neither cavities nor any significant changes of the overall microstructure could be observed.

3.2 Cavitation after four-point bending

Observations were restricted to HP-AlN, deformed at 1873 K. FPB leads in the same sample to areas submitted to tensile stresses while others are in compression. To a good approximation, the stress (tension or compression) in a thin slice parallel to the top and bottom surfaces is practically uniaxial. Thin foils were cut parallel to these surfaces at ~100 μm beneath them. Determining the local plastic strain and stress is not straightforward. Estimates were derived from the crosshead deflection of the testing machine using the formula of Hollenberg *et al.*[2] with a stress exponent of 1·4.[1]

3.2.1 Areas deformed in tension

Plastic strains were approximately equal to 0·5% at σ = 58 MPa, 0·8% at 80 MPa and 2·2% at 109 MPa; these deformations being obtained, respectively, after 85, 110 and 285 min. Two kinds of cavities were observed (Fig. 1). Firstly, at GBs, cavities have lenticular shapes with a thickness, normal to the GB plane, roughly half the diameter in the GB plane. At a given stage of deformation, all cavities have fairly equal sizes (Table 1). And, secondly, at triple junctions, cavities are slightly larger and show concave or convex triangular cross-sections. These two classes can be labelled R and W, respectively, as proposed in Ref. 3. No cavity was ever found inside the grains.

The fraction of GBs and triple junctions where cavitation was present was estimated. Each value given in Table 1 results from counting over 100–300 GBs. The size and number of cavities increase with strain and/or stress. At ϵ = 0·8%, σ = 80 MPa, all grains have at least one cavity at their periphery and evidence of coalescence is observed. The spatial distribution of cavities is clearly anisotropic (Fig. 1) and their density is larger at GBs which are nearly perpendicular to the tensile stress axis. For each GB, the β-angle between the stress axis and the GB plane was determined in two steps:

(i) The α-angle between the stress axis and the trace of the GB in the plane of the foil was measured; α varies between a minimum value α_i and 90°.

(ii) The spectrum of α-values was then converted into β-values assuming that GBs have random orientations and that (as was easily checked) α_i is the minimum β-value. Histograms were thus obtained. For ϵ = 0·5 %, σ = 50 MPa, β varies from 45 to 90° with a maximum at 80°. For ϵ = 0·8%, σ = 80 MPa, as shown on Fig. 2, a marked anisotropy is also observed, with the same maximum and a broader spectrum. For ϵ = 2·2 %, σ = 109 MPa, the distribution is quite similar, with a maximum between 80 and 90°.

Table 1. Cavitation after four-point bending

σ (MPa)	ϵ (%)		*R cavities** Ø (μm)	*R cavities** Grain boundaries with cavities (%)	*W cavities*† Triple points with cavities (%)
58	0·5	T	0·33 (0·03)	20	21
		C	0·29 (0·08)	Very weak	Very weak
80	0·8	T	0·42 (0·09)	30	57
		C	0·37 (0·03)	5	19
109	2·2	T	0·51 (0·34)	48	66
		C	0·54 (0·22)	4	20

*R cavities: diameter (and standard deviation) and percentage of grain boundaries containing cavities are given.
†W cavities: percentage of triple points with cavities is given.
T = Area in tension; C = area in compression.

Fig. 1. Anisotropic cavity distribution in AlN after deformation by four-point bending (tension side) at T = 1873 K, σ = 80 MPa, $\epsilon = 0{\cdot}8 \times 10^{-2}$. The stress axis is parallel to the marker.

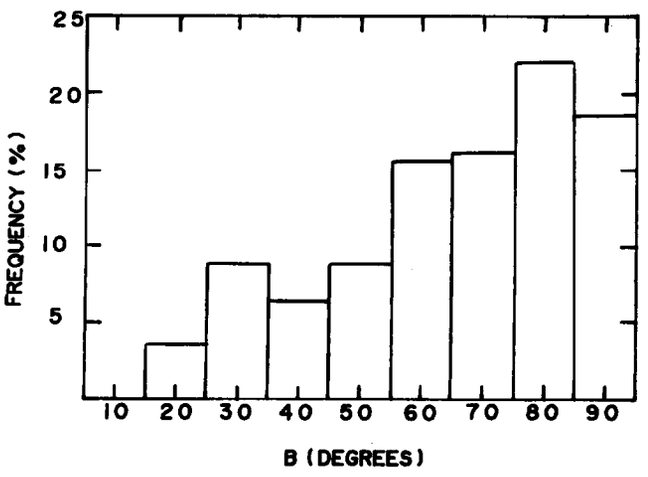

Fig. 2. Anisotropic distribution of cavities after four-point bending (tension side) for same conditions as Fig. 1. Histogram of the β-angle between the stress axis and the grain boundary plane, showing cavities (179 measurements).

3.2.2 Areas deformed in compression

Cavitation is much less developed in compressed areas, whatever the strain, as can be seen in Table 1. Cavities have the same lenticular shape and about the same size as in tension areas. Many GBs do not show cavities but the density of cavities at cavitated GBs is nearly the same as in tension. Cavitated GBs appear to be orientated at random, some being nearly parallel to the stress axis.

A significant observation is that a particle can be seen as a black dot in nearly each cavity. These particles were identified by EDS analysis and microdiffraction. They are crystallized precipitates of sintering additive (La_2O_3). Fig. 3(a) shows a GB orientated at 60° from the foil, so that cavities have elongated shapes. Particles appear at the same side of the cavities. This was not always observed. Particles may occupy diametrically opposite positions and, in a few cases, two or three particles were found in one cavity. In tension areas, in comparison, such particles were seen in a small number of cavities only. It may be mentioned that particles not attached to cavities could be found in some GBs even after 2·4% strain. Fig. 3(b) shows some particles at the GBs of a small AlN grain. The particular contrast marked by the arrow could reveal the beginning of cavitation. Such an observation, however, was extremely rare. Practically no cavities smaller than 0·1 μm were observed either in tension or compression areas in the three samples we have studied. Typically, the apparent size of particles varied from 20 to 100 nm.

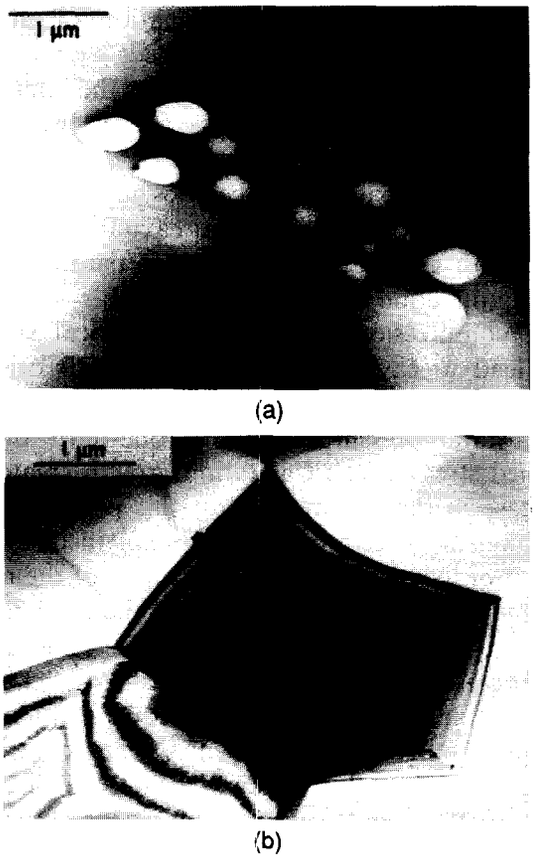

Fig. 3. Cavitation in AlN after deformation by four-point bending (compression side). (a) Cavities formed at second-phase particles in an inclined grain boundary (T = 1873 K, σ = 58 MPa, $\epsilon = 0{\cdot}5 \times 10^{-2}$) viewed using bright field TEM. (b) Second-phase particles around a small grain viewed using bright field TEM. The arrow points to the growth of a cavity (T = 1873 K, σ = 109 MPa, $\epsilon = 2{\cdot}2 \times 10^{-2}$).

3.3 Cavitation after uniaxial compression

A number of creep tests of 10^4 s to 5×10^4 s duration were performed on the two grades of AlN. Tests were interrupted after quasi-stationary creep had been established. The maximum strain attained was ~6%. Some samples were deformed in dynamic compression, under an imposed strain rate chosen in the range of steady state creep rates previously observed. The main results are as follows:

- Intragranular cavitation was never detected.
- Cavitation at GBs, on the contrary, was always observed, even after the smallest strain investigated, i.e. ~0·5%.
- R cavities initially have the lenticular shape described in Section 3.1. When growing, they change to ellipsoids with the major axis in the GB plane, as could be observed at GBs which were at a small angle from the foil plane. The rounded shape is lost for large cavities, which become facetted. The crystallographic orientation of facets could not be determined. Facets obviously depend on the orientation of the two adjacent grains (Fig. 4, marked F).
- The growth of a cavity is not necessarily symmetric inside the two adjacent grains, yet the size of cavities at a given stage of sample deformation is rather homogeneous, as observed after FPB.

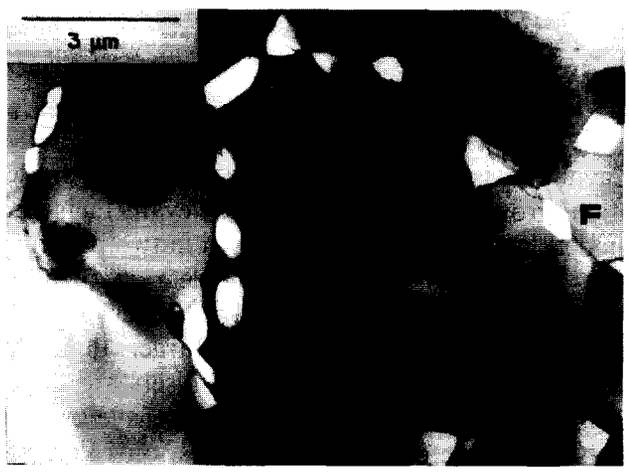

Fig. 4. Facetted cavities (F) in AlN after creep in compression (T = 1873 K, σ = 250 MPa, $\epsilon = 2{\cdot}3 \times 10^{-2}$). Dislocations (D) and one inversion domain boundary (I) can be seen in one grain.

- No clear preferential orientation of cavitated grains could be detected, in spite of observations performed in foils cut at different angles from the stress axis.
- Cavitation does not appear to be correlated with intragranular extended defects, such as dislocations or inversion domain boundaries, which can be seen in Fig. 4.
- Particles like those observed after FPB were seen in a few cavities, especially in smaller ones. It must be pointed out that cavities larger than ~1 μm are usually cut by the two faces of the thin foil, so that existing particles may have disappeared during thinning.

We are not able to state how cavity nucleation and growth are affected by each testing parameter, such as temperature, stress, strain rate and strain. We should mention, however, that the volume fraction of cavities f_v was found to be more or less equal to the total strain, for both grades of AlN, irrespective of other testing conditions. No convincing correlation between the diameter Ø of cavities (before coalescence sets in) and the strain was found. The $f_v / Ø^3$ ratio is proportional to the number of cavities per unit volume. It remains almost constant when strain is increased from 2 to 6%. This means that the number of cavities does not evolve and that the increase in the volume of cavitation is due to the growth of a constant number of cavities instead of a continuous nucleation and growth process. This is consistent with the observation that the size distribution of cavities is rather narrow in a given sample.

W-type cavities have initially the shape of concave triangles and change into convex triangles and three-branch stars as cavitation penetrates along adjacent GBs. Their size is consistently slightly larger than that of R-type cavities.

4 Discussion

Cavitation is a three-step process involving nucleation, growth and coalescence. Relevant facts and models have recently been reviewed in two papers.[4,5]

It is believed that cavity nucleation at GBs requires tensile stresses of the order of 1% of the Young modulus,[6] much larger than the applied stress in any case. Stress raisers are therefore needed, which must also create tensile stresses in samples deformed in compression. Possible stress raisers are GB ledges or second-phase particles, which both prevent GB gliding. In Al_2O_3 samples[7] containing a high density of marked GB ledges, those defects were seen to be preferred sites of cavitation. No such ledges were detected in the present work. Observations of particles acting as cavity nuclei were reported in Cu alloys[8] for large particles (~1 μm diameter), and in AlN[9] and α-SiC[10] for any particles. Here, only small particles were identified as possible nuclei. The role played by such defects was very clear especially after a slight deformation in compression (FPB) when all cavities were nucleated at particles. It is probable that in tension areas, cavitation started at defects too small to be detected by conventional TEM. It may be stressed that the very narrow size distribution of cavities within the same GB points to nearly simultaneous nucleation.

In compressed samples, tensile stresses are always developed at some GBs, especially when GB sliding is impeded by local obstacles. An example can be seen in the Fig. 19a of Ref. 4. A local concentration of tensile stresses may induce decohesion. Stress concentrations were reported by several authors. In TEM, they form patterns of concentric fringes and are called 'whorls'. Such defects are always very rare and could not be characterized. They are probably rather unstable and converted into cavities from the very beginning of deformation. The formation of cavities relaxes local stresses. Once formed, cavities take the lenticular shape which minimizes the interfacial energy, thanks to transport of matter by surface diffusion. The observation that nuclei particles remain on the same axis for all cavities in a given GB is consistent with the view that cavitation is correlated with GB gliding. This axis is parallel to the gliding direction in that particular GB.

In compression, it appears that local stresses can lead to cavitation whatever the GB orientation to the stress axis. In compression tests a hydrostatic pressure equal to one-third of the applied stress exists. Cavitation growth creates an increase in the volume against this pressure. This mechanism is only physically explained by the action of local stresses and in the rest of the material by transformations decreasing the total energy and length of the sample. Further investigation is in progress to clarify this point. As expected, however, cavitation is much more frequent in tension, where the growth of cavities can contribute directly to the total plastic strain. And lastly, it appears that coalescence merely occurs through simultaneous growth of all cavities.

References

1. Masson, I., Feiereisen, J. P., Michel, J. P., George, A., Mocellin, A. & Blumenfeld, P., *J. Eur. Ceram. Soc.*, **13** (1994) 355.

2. Hollenberg, G. W., Terwilliger, G. R. & Gordon, R. S., *J. Eur. Ceram. Soc.*, **54** (1970) 196.
3. Garofalo, F., *Fundamentals of Creep and Creep-Rupture in Metals*. MacMillan Co., New York, 1965, p. 216.
4. Chan, K. S. & Page, R. A., *J. Am. Ceram. Soc.*, **76** (1993) 83.
5. Rodriguez, P. & Bhanu Sankara Rao, K., *Prog. Mater Sci.*, **37** (1993) 403.
6. Page, R. A., Lankford, J. & Spooner, S., *J. Mater. Sci.*, **19** (1984) 3360.
7. Page, R. A., Lankford, J., Chan, K. S., Hardman-Rhyne, K. & Spooner, S., *J. Am. Ceram. Soc.*, **70** (1987) 137.
8. Fleck, R. G., Taplin, D. M. R. & Beevers, C. J., *Acta Metall.*, **23** (1975) 415.
9. Jou, Z. C. & Virkar, A. V., *J. Am. Ceram. Soc.*, **73** (1990) 1928.
10. Carter Jr, C. H., Davis, R. F. & Bentley, J., *J. Am. Ceram. Soc.*, **67** (1984) 409.